WPBB-PR(18) 20113

A. Froio et al.

Parametric thermal-hydraulic analysis of the EU DEMO Water-Cooled Lithium-Lead First Wall using the GETTHEM code

Preprint of Paper to be submitted for publication in
Fusion Engineering and Design

This work has been carried out within the framework of the EUROfusion Consortium and has received funding from the Euratom research and training programme 2014-2018 under grant agreement No 633053. The views and opinions expressed herein do not necessarily reflect those of the European Commission.

Parametric thermal-hydraulic analysis of the EU DEMO Water-Cooled Lithium-Lead First Wall using the GETTHEM code

A. Froio[a]*, A. Del Nevo[b], E. Martelli[b,c], L. Savoldi[a] and R. Zanino[a]

[a]*NEMO group, Dipartimento Energia, Politecnico di Torino, 10129 Torino, Italy*
[b]*ENEA CR Brasimone, 40032 Camugnano, BO, Italy*
[c]*Università di Roma "La Sapienza", 00185 Roma, Italy*
** Corresponding author: antonio.froio@polito.it*

Abstract

The system-level code GETTHEM is applied for the first time to the thermal-hydraulic analysis of an entire segment of the Water-Cooled Lithium-Lead (WCLL) Breeding Blanket First Wall (FW) of the EU DEMO reactor, parametrically varying the heat load on the FW and the coolant mass flow rate. The results show that the WCLL FW is generally safe with respect to variations of the applied heat flux with respect to the design value, if the average heat load conditions are considered. A further analysis is then performed, identifying the top inboard region and the bottom outboard region as the most critical points from the point of view of the refrigeration of the FW. Finally, the largest possible extent of the WCLL FW surface where the peak heat load can be safely applied is identified through a parametric analysis, performed on the critical regions identified above.

Keywords

Nuclear fusion, EU DEMO, breeding blanket, WCLL, first wall, thermal-hydraulics, modelling

1. Introduction

One of the challenges of a DEMO reactor is the efficient removal of the heat deposited in the blanket First Wall (FW) by means of a heat transfer fluid, which should heat up to produce turbine-grade vapour in a steam generator for the production of electricity. The EU DEMO reactor, see Figure 1a, which aims at producing net electrical energy from nuclear fusion by 2050 [1], foresees in its current pre-conceptual design phase different possible solutions for the blanket, which couple different concepts of Breeding Zone (BZ) to different concepts for the heat removal from the FW. In all cases, the blanket is divided into 18 sectors (according to the 2015 design revision); each sector contains three Outboard (OB) and two Inboard (IB) blanket segments, see Figure 1b-c, resulting in a total of 54 OB and 36 IB segments, respectively.

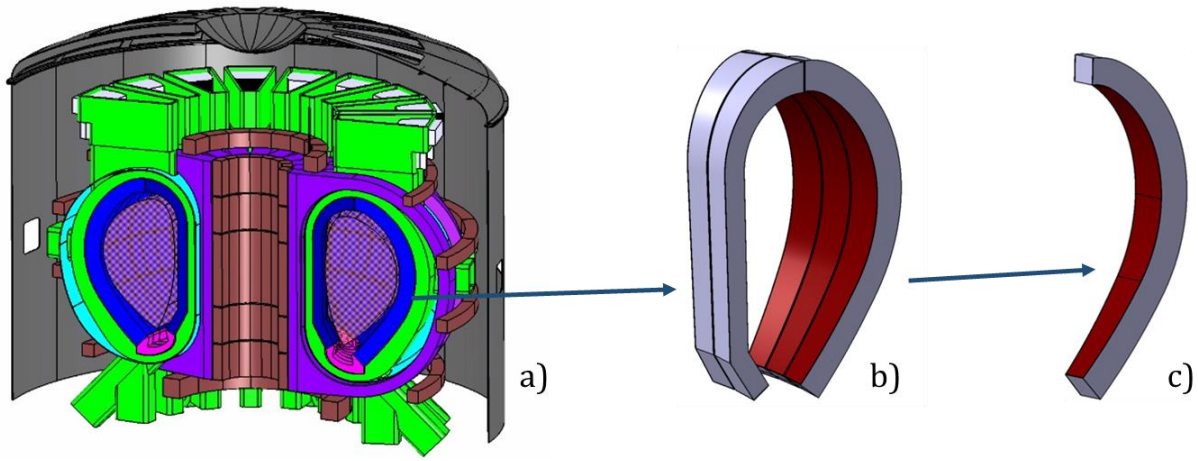

Figure 1: a) the 2015 revision of the EU DEMO design; b) one blanket sector; c) one blanket (outboard) segment (reproduced or adapted from [2, 3]).

Among the different alternatives, the Water-Cooled Lithium-Lead (WCLL) [3] Breeding Blanket (BB) concept uses water in standard Pressurized Water Reactor conditions (i.e. 155 bar operating pressure of the coolant, 295-328 °C inlet-outlet temperature) to cool both BZ and FW, using two fully independent Primary Heat Transfer Systems (PHTS) [4]. The design mass flow rate distribution among the channels in the different elementary units is determined through an energy balance, starting from the nuclear heat load to the BZ as computed through neutronic analyses, plus a uniform heat flux of 290 kW/m² on the FW surface[1], in order to achieve the design outlet temperature in all cooling channels.

In order to verify the suitability of the design, the detailed check of the compatibility of the materials (and namely the EUROFER temperature, to be kept at T < 550 °C [5]) with the hot-spot temperature $T_{hotspot}$ foreseen in the BB has been performed by means of 3D Computational Fluid Dynamic (CFD) analyses just on one elementary unit located in the OB equatorial region [3]: in view of the huge computational cost of the CFD analyses, a similar check, but for the entire BB, is not viable. However, the assessment of $T_{hotspot}$ for all modules is needed, as well as the check of the effects of the deviation of the heat load from the reference value.

Motivated by the considerations above, the GEneral Tokamak THErmal-hydraulic Model (GETTHEM) has been recently developed [6, 7], with the support of the EUROfusion Programme Management Unit, to perform fast system-level thermal-hydraulic transient analyses of the PHTS. As a first application, the code was used for the evaluation of $T_{hotspot}$ in the Helium-Cooled Pebble Bed BB [8], while the model for the cooling loops of one elementary unit of the WCLL BB was developed and benchmarked against available CFD simulations [7]. It becomes therefore natural, at this stage, to extend it to the entire segment.

[1] This was the design value assumed until 2016 for all the EU DEMO BB concepts.

In the present paper, after a brief description of the WCLL FW current design and of the corresponding GETTHEM model, as well as of the reference heat load map on the FW, the GETTHEM model of an entire segment of the WCLL FW is used to evaluate the $T_{hotspot}$ in the entire EUROFER structure and check it against the mentioned 550 °C limit. Parametric thermal-hydraulic analyses, considering the latest FW average heat load specification and different mass flow rate values, are then performed; finally, the peak heat load specification is applied to increasingly larger portions of the FW, to evaluate the largest surface where the peak heat flux can be applied without overcoming 550 °C in the EUROFER, aiming at the identification of the cooling limits of the WCLL FW.

2. The WCLL First Wall Design

The current design of the WCLL BB is based on the Single Module Segment (SMS) approach: each blanket segment is a continuous structure, see Figure 1c and Figure 2, where the stiffening grids are also shown.

The pre-conceptual design of the WCLL BB is based on a repetitive structure, where the same elementary unit (shown in Figure 3), containing 21 BZ cooling tubes and 10 FW cooling channels, is repeated in the poloidal direction; the elementary units are separated by the toroidal-radial stiffening plates.

The BZ is cooled using double-wall tubes (a sandwich of EUROFER-copper-EUROFER), to reduce the risk of interaction between the LiPb, flowing outside the tubes, and water, flowing inside the tubes. The cross section of a portion of the WCLL FW (related to the bottom edge of the OB segment) is reported in Figure 3c. The FW is made of EUROFER, and the plasma-facing wall is covered with a 2-mm thick tungsten layer. On the internal side, the EUROFER is in direct contact with the PbLi in the BZ. The FW cooling channels are square, see Figure 3, with a side of 7 mm and a pitch of 13.5 mm; the coolant is distributed to (and collected from) the cooling channels by manifolds in the segment Back Supporting Structure (BSS), see Figure 2b, designed in such a way that the flow in adjacent channels is always in counter-current. All FW cooling channels in the machine are connected to the same loop [4], through the manifolds in the BSS, see Figure 2b.

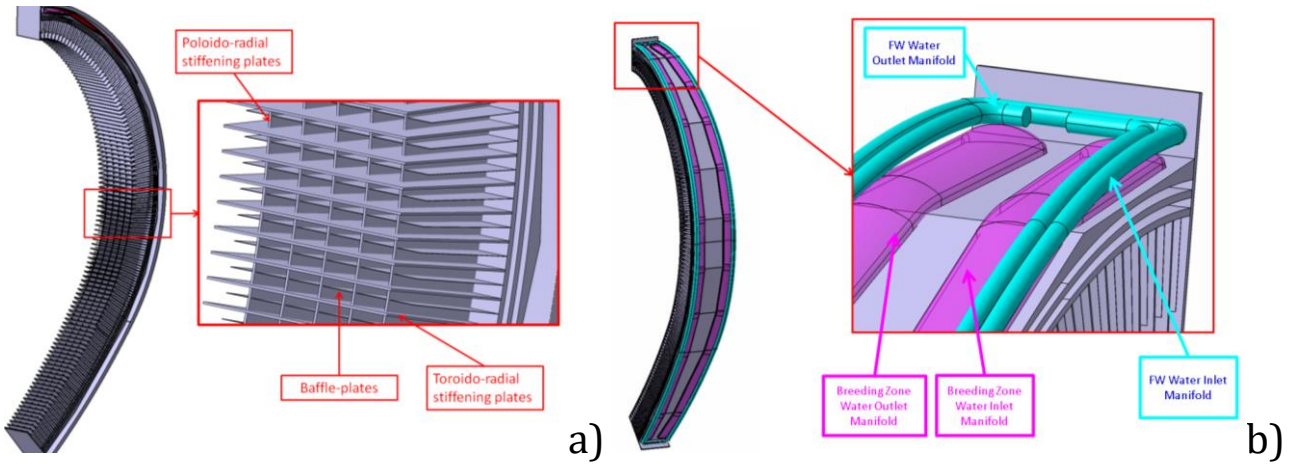

Figure 2: Schematic view of a WCLL segment (reproduced from [3]). (a) Front view, with the detail of the stiffening grids, and (b) rear view (BSS), with the inlet and outlet manifolds for the FW and BZ coolant.

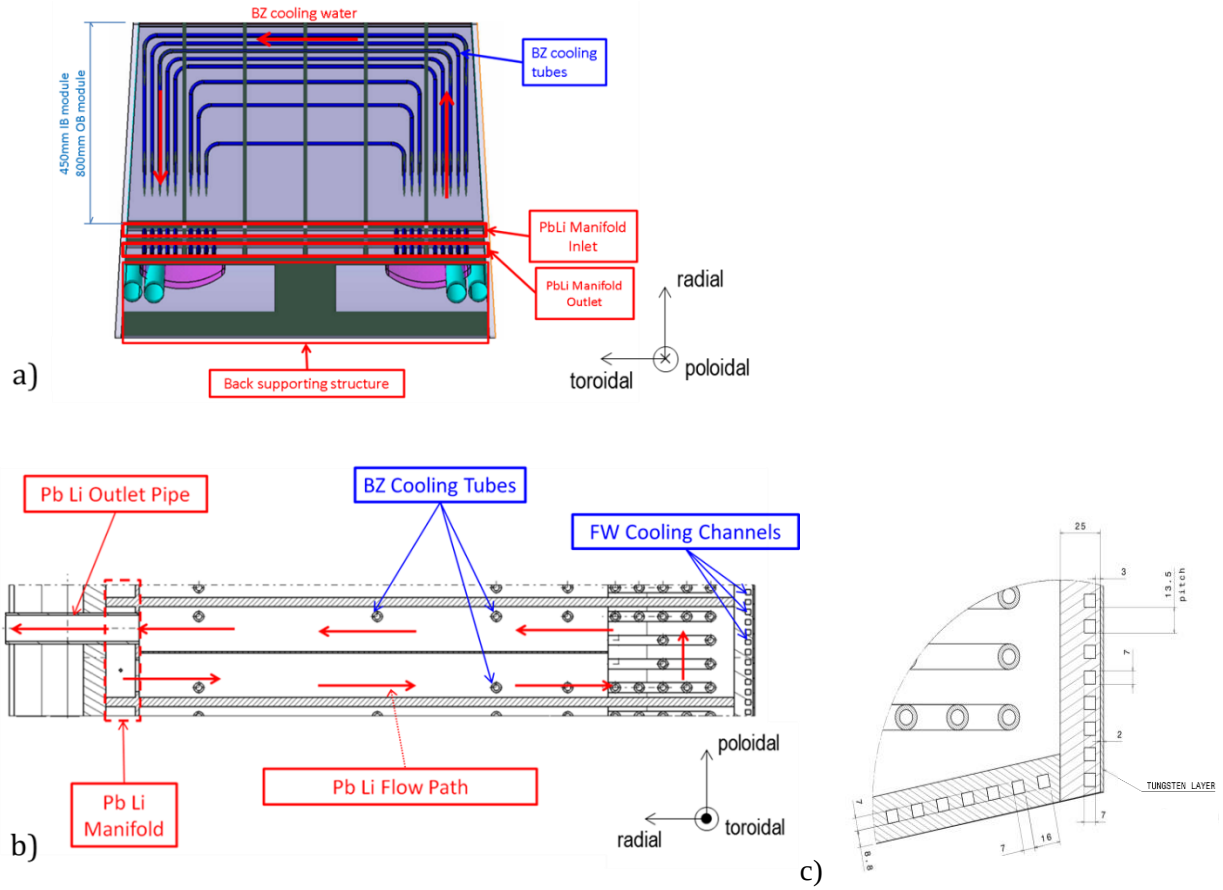

Figure 3: Radial-toroidal (a) and radial-poloidal (b) views of a WCLL elementary unit. (c) Detail of the cross section of the FW, showing the bottom edge of the OB segment, with the square cooling channels (reproduced from [3]).

3. The GETTHEM WCLL First Wall cooling system model

In the GETTHEM model of the WCLL, two different PHTSs are modelled for the water: the FW PHTS and, separately, the BZ PHTS (details on the GETTHEM models can be found in [6, 7, 8]); we focus here on the FW, without modelling the ex-vessel components (fixed pressure at the segment inlet and outlet are assumed). The FW is discretized in a number of objects equal to the number of FW channels and including the corresponding volume of EUROFER, as shown in Figure 4. Adjacent channels are thermally coupled through the thermal resistance of the solid in between, see below, while the two solid volumes belonging to neighbouring objects are assumed to be in perfect thermal contact. Each object is discretized in finite volumes (see also Figure 4), which then allow finding an approximate solution of a coupled set of 1D (along the flow direction), transient nonlinear partial differential equations including:

- the mass, momentum and energy conservation laws, for the fluid;
- the heat conduction, for the solid.

As a system-level model, GETTHEM can directly compute only average temperatures in the finite volumes; so, a procedure has been developed to estimate the hot-spot temperature in the EUROFER in the postprocessing phase, which is resumed in the Appendix.

For the code to be fast-running, the water coolant is modelled always as a single-phase liquid[2] (no boiling is accounted for), with linearized thermo-physical properties (specific heat, density and internal energy derivative with respect to the temperature) in the entire operational range of the BB (155 bar, 295-328 °C);

[2] This assumption is consistent, if taking into account that boiling is not foreseen during normal operation. For off-normal analyses, this assumption is relieved in the GETTHEM model (see [12]).

also, the thermo-physical properties of the EUROFER are assumed constant and equal to the average values in the temperature range of interest (295-550 °C). The heat transfer coefficient (HTC) between solid and liquid is also taken as a constant, i.e., the average HTC computed with the Dittus-Bölter correlation in the operational range. It has been estimated (through dedicated simulations, comparing GETTHEM results against detailed models) that all these assumptions produce an error below 3 % in terms of temperature for steady-state analyses, as in this case.

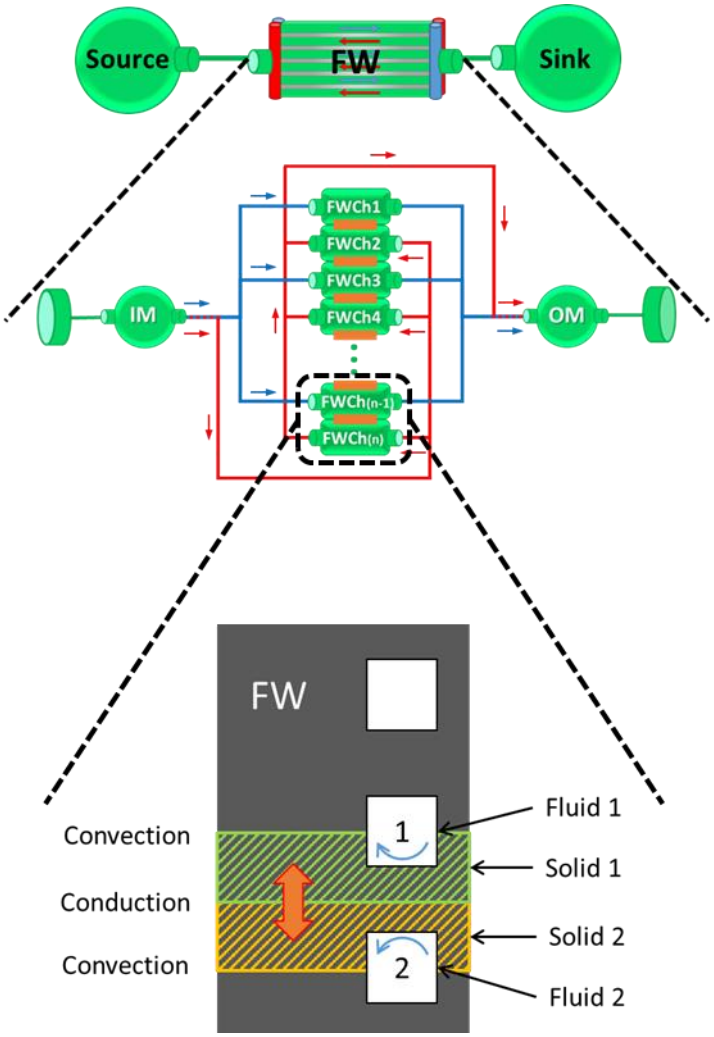

Figure 4: Sketch of the GETTHEM WCLL FW PHTS model, showing the detail of the FW component and the heat transfer mechanisms accounted for in the solid finite volumes (IM/OM: Inlet/Outlet Manifold).

4. Scenarios

The different scenarios analysed in the present paper are obtained combining different possible choices as far as the heat load, mass flow rate and coolant HTC are concerned, as explained below.

The simulations are driven by the nuclear heat load, acting on both FW (the so-called Nuclear Wall Load, NWL) and BZ, and the heat load coming from the plasma, acting on the FW.

In the absence of more recent neutronic analyses, the NWL is assumed equal to that computed in [9].

For the plasma heat load, the most recent poloidal distribution provided by the EUROfusion Programme Management Unit (PMU) [10] is used[3]. This heat flux distribution is however determined based on a FW

[3] Note that this is not the input used for the design of the WCLL, which is instead a uniform heat flux of 290 kW/m², as mentioned above.

configuration (reported in Figure 5a) which is somewhat different from the WCLL one, i.e. having a different poloidal shape, a multi-module segment approach and also a central OB segment different from the other two, being based on the 2017 EU DEMO1 design. To overcome this issue, the heat load to the FW is rescaled, for the sake of the analysis presented in this paper, distributing the different heat loads on the portions of the WCLL single-module segment FW corresponding to the different modules, as shown in Figure 5b. Since the OB segments in the WCLL design are all identical, the total power on the three "PMU" segments has been simply divided by 3, to obtain a heat flux related to the "average" segment. Those are of course very rough assumptions, as the heat load coming from the plasma is strongly anisotropic and depends heavily on the FW shape itself. Indeed, as clearly stated in [10], the FW heat load specification computed by the PMU can be considered valid only for the 2017 EU DEMO1 FW shape. Nevertheless, the aim of this work is *not* to determine what would be the correct heat load distribution, but to analyse the robustness of the design of the WCLL cooling system, i.e. to identify how much a deviation in the heat load from the design specification would affect the cooling performance; consequently, this "roughly reshaped" heat load distribution is used in the present work. The resulting heat flux distribution is reported in Figure 6. In [10], in addition to the average heat flux, also the peak value is reported, which can be deposited on small portions of the FW (without affecting the total power deposition); these peak values are shown in Figure 6 as well.

Looking at Figure 6, it is evident that the heat flux distribution among the modules is highly nonuniform, with the largest loads on the top and bottom parts of the FW (Mods. 1, 6-8 and especially 15); on the FW of Mod. 6 the peak heat flux reaches almost 1.4 MW/m², which is ~5× larger than the 0.29 MW/m² design value. When applying the PMU average heat flux, the total power to the entire segment increases with respect to the WCLL design value by ~25 % on the IB (going from 3.26 MW to 4.08 MW) and by ~19 % on the OB (from 6.49 MW to 7.71 MW).

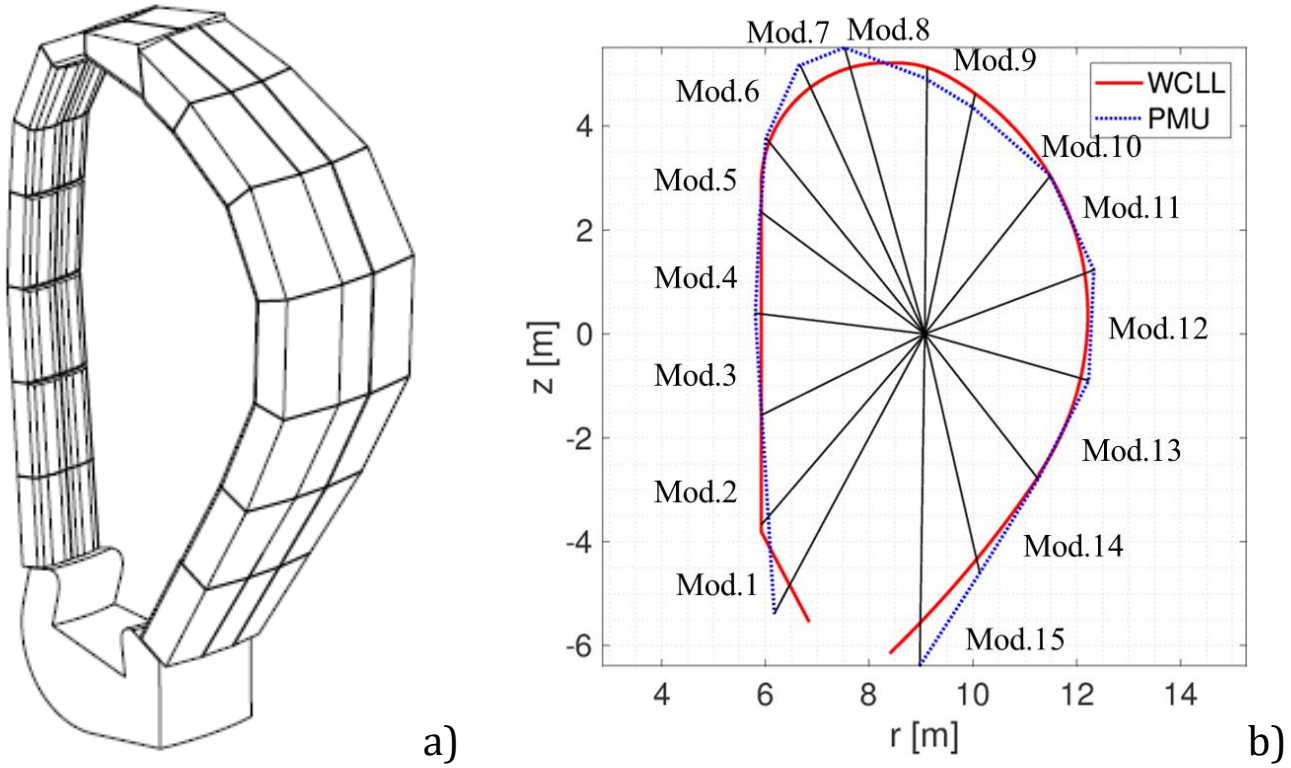

Figure 5: (a) 3D FW geometry used by the EUROfusion PMU to compute the plasma heat flux [11]. (b) Comparison of the poloidal profiles of the WCLL (solid line) and PMU (dashed line) FWs; the poloidal profile of the PMU FW refers to the middle of the central OB segment, whereas the WCLL one is the same for all toroidal locations.

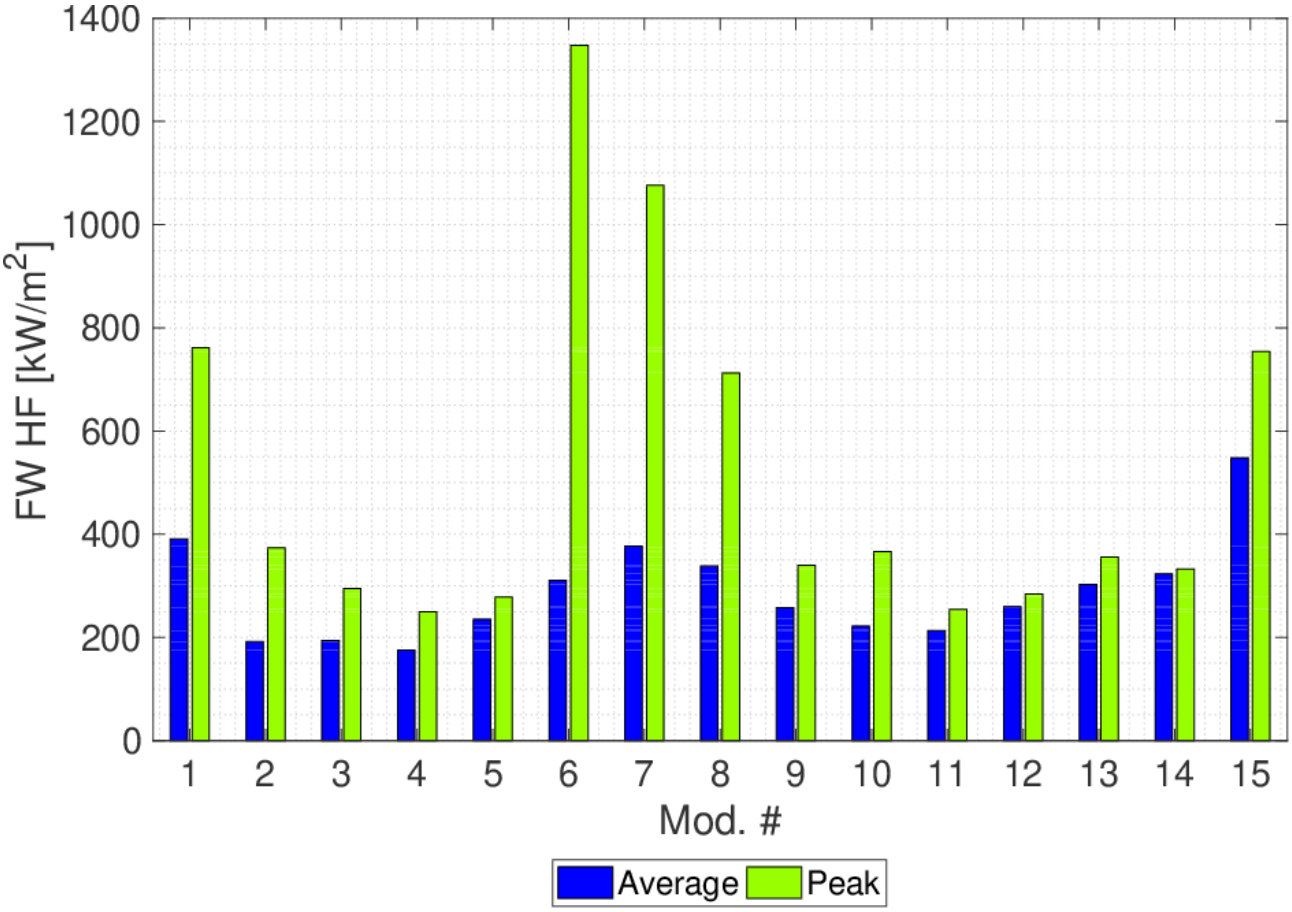

Figure 6: Average and peak plasma heat flux to the FW surface.

As far as the coolant mass flow rate is concerned, different alternatives are considered:

- the WCLL design distribution;
- a mass flow rate distributed according to the PMU average heat flux, keeping the total mass flow rate equal to the WCLL design value;
- a mass flow rate distribution computed in order to have a uniform outlet temperature, equal to the design value of 328 °C, according to equation (1).

As far as the HTC is concerned, as already mentioned, the average HTC is computed in the temperature range (295-328 °C); then, the minimum value among all the channels (according to the different mass flow rates) is used for the entire segment (with the exception of one scenario, where the average value is used, as explained below).

The different scenarios considered in the present paper are summarized in Table 1; the distribution of the relevant parameters (heat load, HTC and mass flow rate) in Scenarios 1-4 is also reported in Figure 7.

In Scenarios 1 and 2 the effect of different HTCs is investigated: the average value among all the channels in the segment is used in Scenario 1, whereas the minimum value is used in Scenario 2 (conservative assumption).

In Scenario 3, the same total mass flow rate is used, but it is redistributed to the channels according to the PMU average power distribution, in order to have a uniform outlet temperature. In Scenario 4, also the total mass flow rate is changed according to

$$\dot{m}_i = \frac{\dot{Q}_i}{h_{out} - h_{in}} \tag{1}$$

where $\dot{m}_i$ is the mass flow rate in the *i*-th channel, $\dot{Q}$ is the power deposited in the *i*-th channel, h_{out} is the outlet enthalpy at 328 °C and h_{in} is the inlet enthalpy at 295 °C), so that the outlet temperature distribution is uniformly equal to the design value (328 °C). The aim is to have here a base case, which keeps the structures at a safe temperature, while at the same time allowing the Balance-of-Plant to work in its design conditions.

Finally, keeping the mass flow rate distribution as in Scenario 4, a parametric analysis is performed, applying the peak heat flux only to an increasing number of channels in each region (uniformly on the channel length), until the T_{hotspot} overcomes 550 °C.

Finally, the scenarios described here are modelled as steady-state, as these loads are constant during the plasma burn phase, which lasts much longer than the characteristic times of the cooling system, see [6, 8] and references therein.

Table 1: List of the analyzed scenarios.

Scenario	**Mass flow rate**	**Heat load distribution**	**HTC**
1	Total value and distribution according to design data	According to PMU average HF	**Average** value
2	Total value and distribution according to design data		**Minimum** value
3	Total value according to design data, distribution according to PMU power specifications		
4	Total value and distribution recalculated according to PMU power specifications		

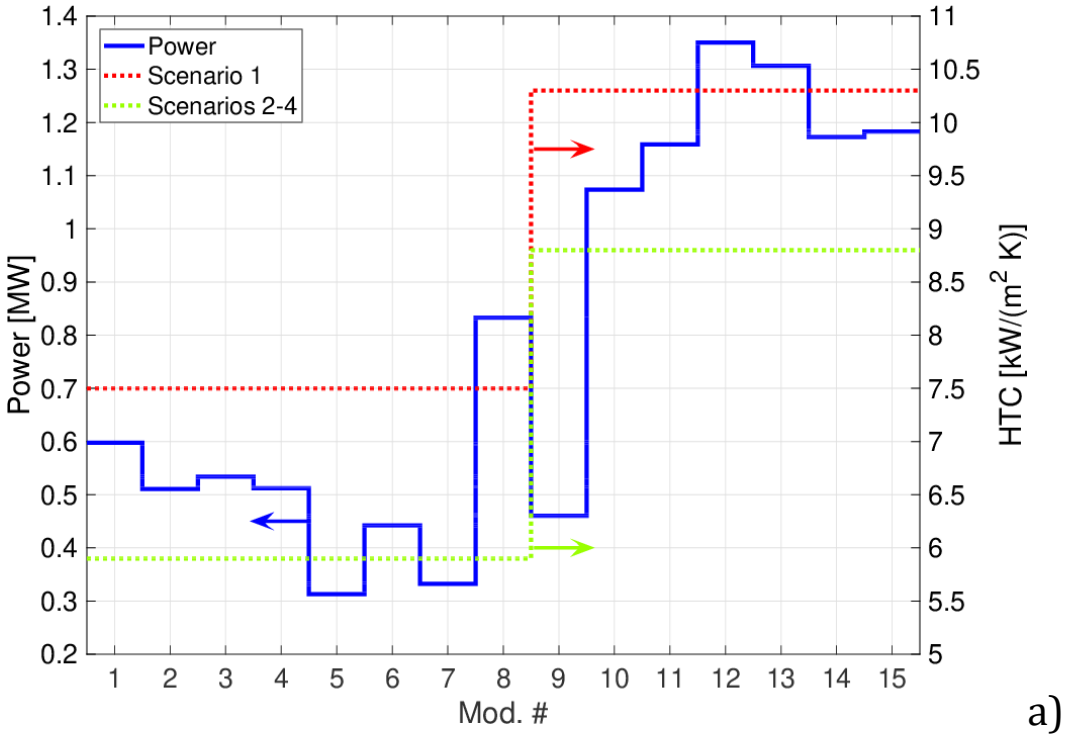

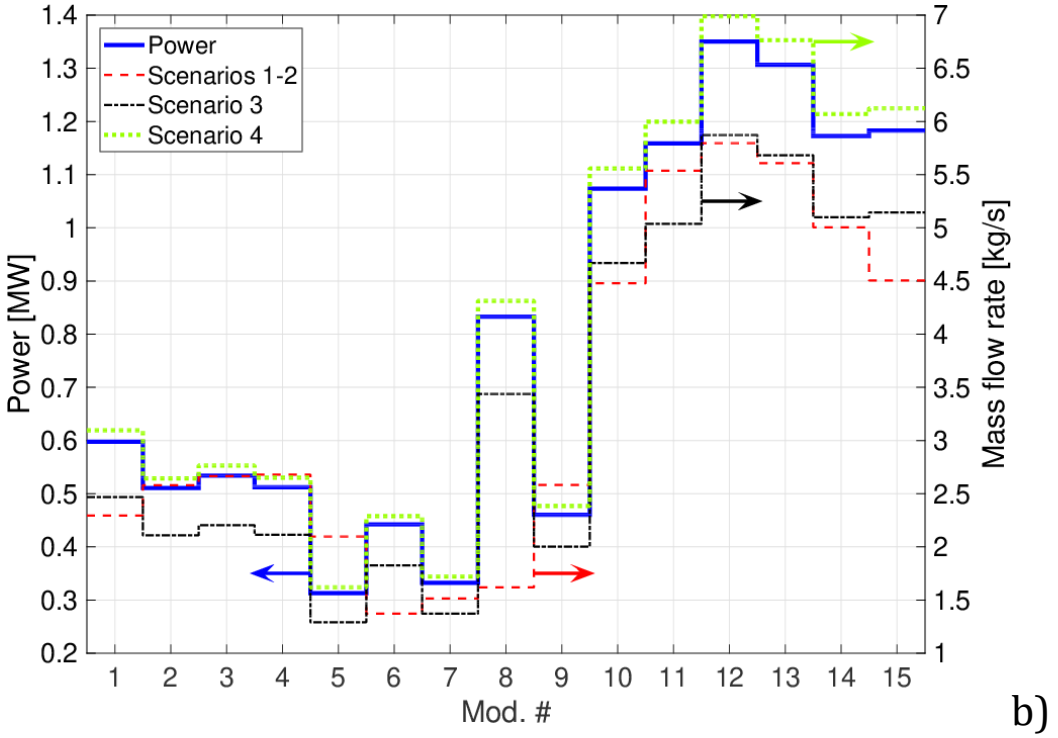

Figure 7: Poloidal distribution of total heat load (solid lines, left axes), HTC (dashed lines, right axis in a) and mass flow rate (dashed lines, right axis in b) for all the scenarios analyzed in this work.

5. Results

5.1. Scenarios 1-4

Figure 8 reports the distribution of the $T_{hotspot}$ in a WCLL FW segment, for the four scenarios. As expected, the most critical point is in the region of Mod. 8, where the heat flux (and total power, consequently) causes an overheating of the structures; nevertheless, the $T_{hotspot}$ never overcomes the limit, not even when using the design mass flow rate distribution, and is always below 450 °C. For Scenarios 1-2, the model computes in

Mod. 6 and Mod. 8 a temperature larger than the water saturation temperature at the given pressure, so that its predictions are inaccurate, albeit conservative[4]. In Scenarios 3-4, instead, both IB and OB segments are safely below the temperature limit in all the points, with Mod. 6 and Mod. 8 still containing the hot-spots, and also independent of two-phase flow, as the computed temperature never reaches saturation. In these cases, moreover, the outlet temperature is uniform, see Figure 9, as expected since the mass flow rate distribution has been adapted to the power distribution.

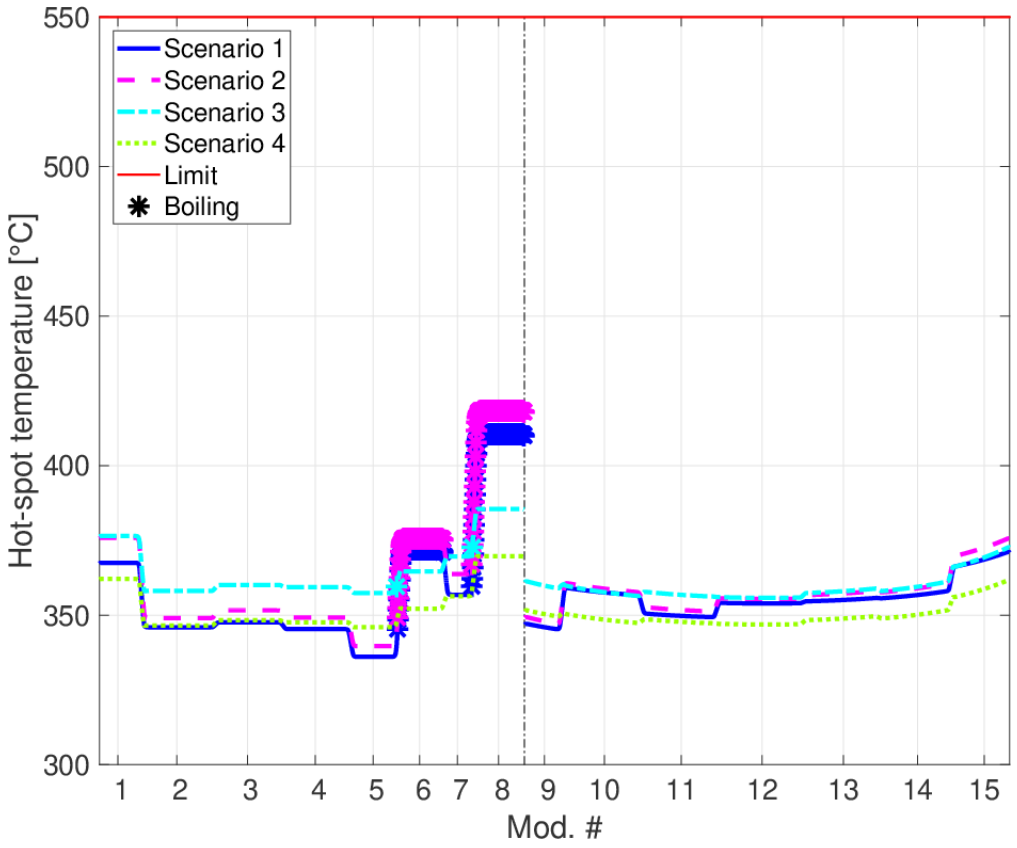

Figure 8: Poloidal distribution of the hotspot temperature for Scenarios 1-4. The thin, red line represents the 550 °C limit; points marked with a star represent a poloidal position corresponding to channels where boiling was detected by the model.

More in detail, the comparison of Scenarios 1-2 shows that the conservative assumption on the HTC causes a modest increase of $T_{hotspot}$ (~7 %); moreover, both IB and OB segments have in all scenarios a large margin with respect to the temperature limit, always above 100 °C. Also, as the total power is more uniform on the OB, the $T_{hotspot}$ distribution is almost uniform at ~350 °C, with only Mod. 15 reaching higher temperatures due to the larger heat flux.

In all four scenarios, the FW temperature distribution is almost piecewise constant in the IB, whereas it has an "average concavity" in the OB: this is caused by the larger thermal conductance of the thermal resistances coupling the different solid models in the OB, driven by the different geometry, which causes nearby modules to affect each other. This effect is also present in the IB, but the curvature is less visible due to the smaller values of thermal conductance.

If the mass flow rate is adapted according to equation (1) in order to match the new total power (and the related distribution), as in Scenario 4, the entire BB is below the operational limit by at least ~170 °C everywhere; this is also compliant with the Balance-of-Plant design, as the outlet temperature is now

[4] Such predictions are in fact not assuming constant fluid temperature in the bulk while boiling, nor considering the increase of HTC associated with boiling.

everywhere equal to the design value of 328 °C (Figure 9). For this reason, this scenario is assumed as a reference case for the parametric analysis.

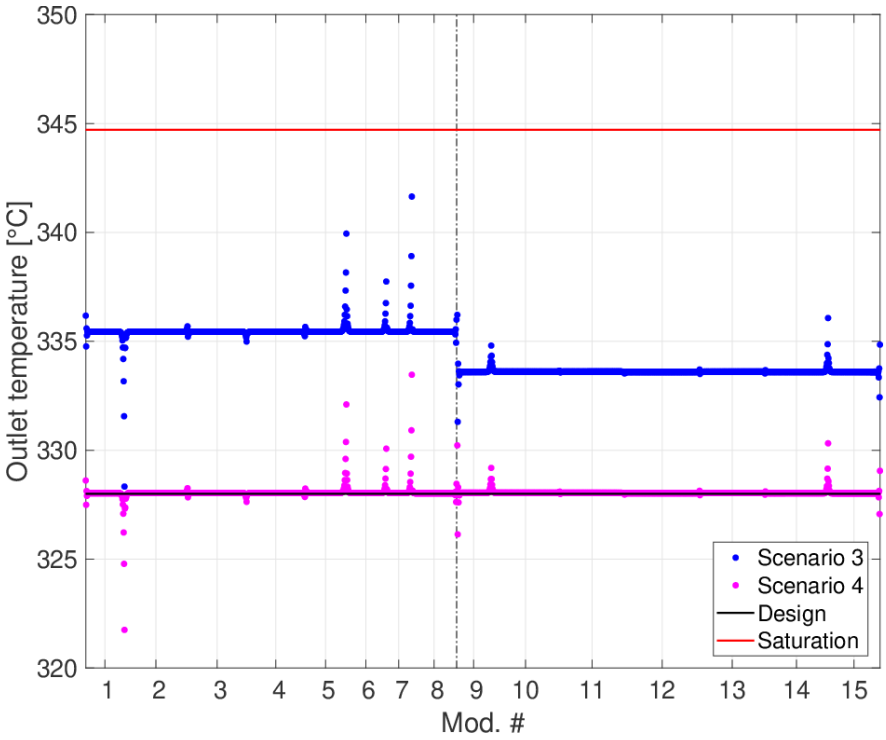

Figure 9: Poloidal distribution of the outlet temperature from the WCLL FW cooling channels, for Scenarios 3 and 4. The thin, red line represents the saturation temperature, whereas the thin, black line represents the design outlet temperature (328 °C).

5.2. Parametric analysis

Starting from the new baseline scenario, identified as Scenario 4 above, the peak heat flux (keeping the NWL constant) is applied on the WCLL FW, in order to identify the largest possible surface which can be loaded with this value, without causing overheating above 550 °C. Since the total power generated in the plasma is kept constant, when applying this peak heat flux to some channels, the heat load to the other channels is reduced.

Before this parametric analysis is performed, however, an *overconservative* scenario is considered, where the peak heat flux is applied to the *entire* BB (keeping the mass flow rate as in Scenario 4); in this case it is not possible to keep the total power constant, so, considering the peak heat fluxes reported in Figure 6 above, the total power is 9.02 MW on the OB and 7.41 MW on the IB, i.e. +20 % on the OB and +80 % on the IB with respect to the design value. Looking at Figure 6 (and considering the results of the previous scenarios), the most critical points are in Mod. 1, 6-8 for IB and Mod. 15 for the OB, where the peak heat flux is much larger than the average value. The aim of such scenario is to immediately identify the most critical points, where the parametric analysis will then focus.

The result of this case is reported in Figure 10 (temperatures above 800 °C are cut in the figure, as they refer to channels where saturation temperature is largely overcome and the GETTHEM predictions are not reliable): also in this overconservative scenario, all the regions (apart from the critical points identified above) show a EUROFER temperature below 420 °C, with ~130 °C of margin at least; nevertheless, boiling is detected in Mod. 2 and 10, meaning that further, detailed investigations are advised in those regions. As expected, the temperature limit is overcome in the IB critical regions, largely in the top portion, where the GETTHEM predictions are nevertheless inaccurate, but also in Mod. 1 by slightly more than 50 °C (also in this case, however, boiling is detected). All the OB points are instead safe, with the exception of the last 14

channels of Mod. 15: however, it should be noted that the peak temperature computed in this region is 558 °C, i.e. ~3 % larger than the temperature limit, which is comparable with the GETTHEM average error estimation as mentioned in section 3 above.

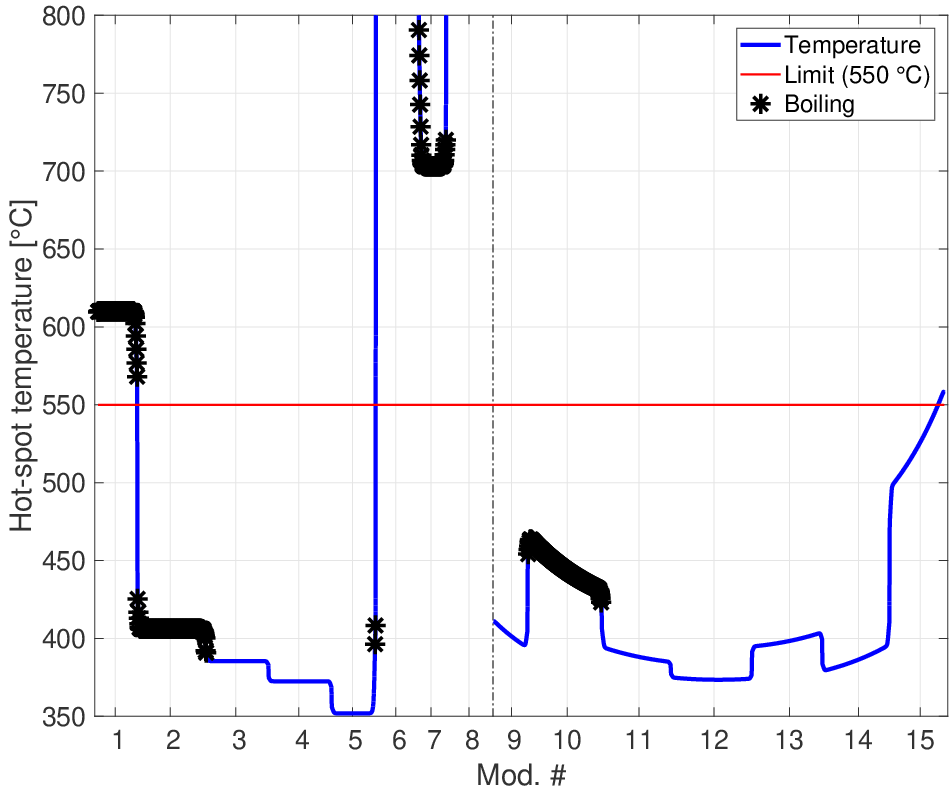

Figure 10: Poloidal distribution of the hotspot temperature, when applying the peak heat flux to the entire BB. The thin, red line represents the 550 °C limit; points marked with a black star represent a poloidal position corresponding to channels where boiling was detected by the model.

The peak heat flux is now applied to an increasing number of channels (uniformly distributed along the plasma-facing channel length) in the regions of Mod. 1-2, 6-8, 10 and 15, to understand what should be the maximum extent of the region which could be "safely" subject to the peak flux (i.e., keeping the EUROFER temperature below the limit or the maximum fluid temperature below saturation). The peak heat flux is imposed in channels in the middle of the region, with the exception of Mod. 15 where the last channels (i.e. the bottom ones) are loaded with the peak value, as they are expected to be more critical (see Figure 8 and Figure 10 above). The results of this analysis are reported in Table 2: the most critical region is found to be Mod. 6, which is unsurprising as the peak heat flux in that region is ~1.4 MW/m². In this region, in fact, both conditions (coolant saturation temperature and EUROFER temperature limit) are met even if a single channel (corresponding to ~0.013 m² of FW surface) is loaded with the peak heat flux. The result is not much different in Mod. 8, where the EUROFER temperature overcomes 550 °C also when loading a single channel, and saturation conditions are detected when two channels (corresponding to ~0.026 m² of FW surface) are loaded. The situation is not better in the other IB regions under investigation, as it is sufficient to load five channels (~0.065 m² of FW surface) with the peak heat flux to reach at least one of the two conditions (in Mod. 2 the hot-spot temperature never overcomes 550 °C, as already highlighted in Figure 10 above).

Coming to the OB, as expected from the previous results a better performance is found: in Mod. 10, which did not reach the EUROFER limit even in the overconservative scenario, saturation conditions are found when loading at least 8 channels (~0.15 m²) with the peak heat flux. In Mod. 15, instead, boiling conditions are never found (as highlighted also in Figure 10), and the EUROFER limit is overcome in the last channel (by 0.7 °C), when the last 9 channels (~0.11 m²) are loaded with the peak heat flux. As already discussed, however, the

safety condition is not met only in a very small portion of the OB segment, and the hot-spot temperature reached is only marginally above the limit.

Table 2: Results of the parametric analysis.

Region	Number of channels loaded with peak heat flux which cause:	
	Boiling	$T_{hotspot}$ **> 550 °C**
Mod. 1	3	6
Mod. 2	5	-
Mod. 6	1	1
Mod. 7	2	4
Mod. 8	2	1
Mod. 10	8	-
Mod. 15	-	9

6. Conclusions and perspective

The GETTHEM system-level transient thermal-hydraulic code has been applied here to analyse the hot-spot temperature distribution in the WCLL BB FW. The most recent FW heat flux distribution, as computed by the EUROfusion PMU, has been rescaled and adapted to the 2016 WCLL design, and applied to the WCLL FW, considering different distributions of the mass flow rate.

The analysis showed that the WCLL design is flexible enough to guarantee adequate cooling of the FW with minor modifications still allowing to keep the coolant outlet temperature at the design value. On the other hand, a parametric analysis with the peak heat flux showed that most of the BB is safe even if loaded with a much larger total power, with the exception of the most critical IB regions far from the equatorial plane.

In perspective, the results of our analysis motivate the need for more detailed (e.g. CFD) studies in the most critical regions; such studies are currently being performed by the WCLL design team. Exploiting the result of such simulations, the GETTHEM approach to the computation of the hot-spot temperature, which depends entirely on previous CFD results, may be improved.

Acknowledgements

This work has been carried out within the framework of the EUROfusion Consortium and has received funding from the Euratom research and training programme 2014-2018 under grant agreement No 633053. The views and opinions expressed herein do not necessarily reflect those of the European Commission.

Appendix: Evaluation of $T_{hotspot}$

GETTHEM computes the average temperature value of each solid finite volume. A more accurate estimate of $T_{hotspot}$ can be obtained through the evaluation of a "peaking factor" f_p^{CFD}, which can be obtained in turn by 3D CFD studies on the elementary unit, see Figure 11. The adopted procedure, already successfully benchmarked and applied to the HCPB [8], is sketched in the flowchart reported in Figure 12.

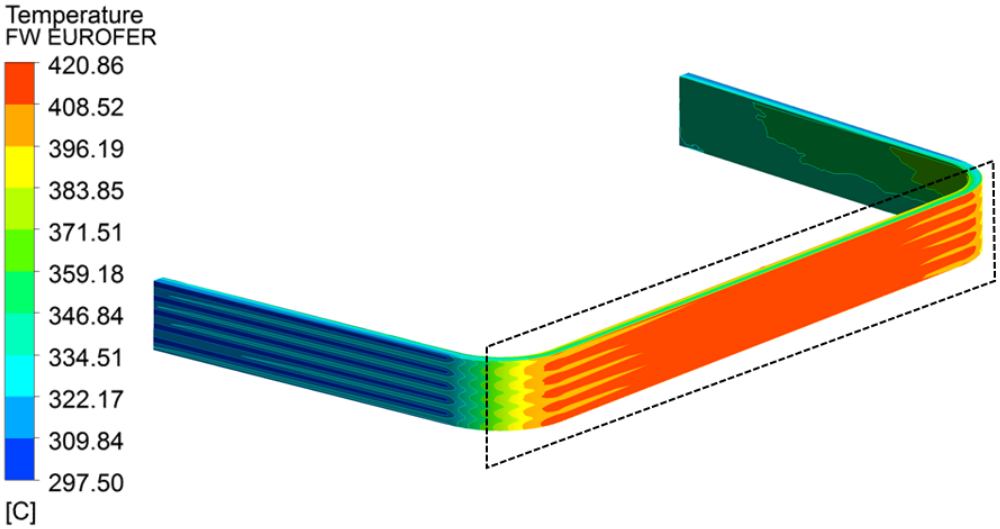

Figure 11: Temperature map on the FW surface, according to the 3D CFD study. The dashed rectangle indicates the region used to determine the peaking factor.

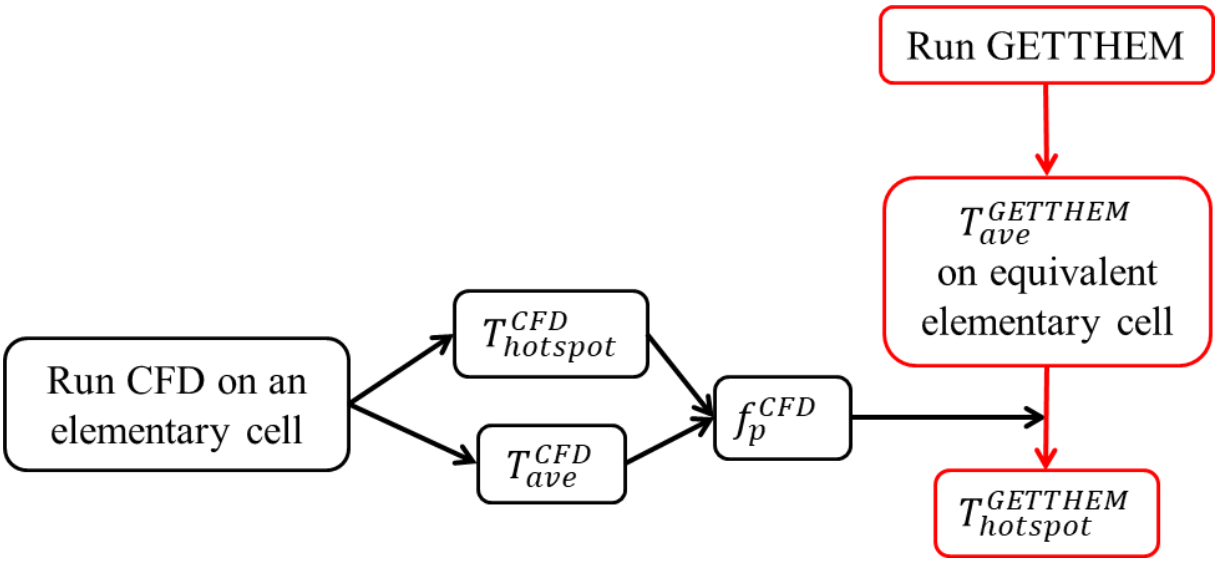

Figure 12: Flow chart for the estimation of the EUROFER hotspot temperature.

Starting from the left part of the flowchart in Figure 12, the value of f_p^{CFD} is computed from the post-processing of the CFD results on an elementary cell, which includes 10 channels, according to

$$f_p^{CFD} = \frac{T_{hotspot}^{CFD} - T_{H_2O,in}}{T_{ave}^{CFD} - T_{H_2O,in}} \quad (2)$$

where $T_{hotspot}^{CFD}$ is the computed hotspot temperature in the EUROFER computational domain, T_{ave}^{CFD} is the volume-averaged temperature in the EUROFER domain (limited to the FW and excluding the side walls, see dashed region in Figure 11) and $T_{H_2O,in}$ is the water inlet temperature (295 °C), taken as a reference temperature. In order to take into account the steeper temperature gradient deriving from a larger heat flux, different CFD simulations have been performed, keeping all the parameters constant (i.e. geometry and coolant mass flow rate) except the heat flux on the FW, which has been varied in the range 200÷1200 kW/m². From these results, a linear correlation for f_p^{CFD} has been obtained as

$$f_p^{CFD}(q'') = 1.58 \times q'' + 0.960 \quad (3)$$

with q'' in MW/m², which best fits the CFD-computed values, see Figure 13. The value of the peaking factor was also checked to be (almost) independent from the value of the mass flow rate: in fact, for different simulations with the same geometry and heat flux, varying the mass flow rate in the range 10 g/s – 25 g/s per channel, the peaking factor changes by <5 %.

As sketched in the right part in Figure 12, the hotspot temperature $T_{hotspot}^{GETTHEM}$ can then be estimated postprocessing the GETTHEM results according to

$$T_{hotspot}^{GETTHEM} = T_{H_2O,in} + f_p^{CFD}\left(T_{ave}^{GETTHEM} - T_{H_2O,in}\right) \tag{4}$$

where $T_{ave}^{GETTHEM}$ is the temperature computed in the FW solid finite volumes by GETTHEM, averaged in 10 adjacent channels to be consistent with the CFD studies on which f_p^{CFD} is based on.

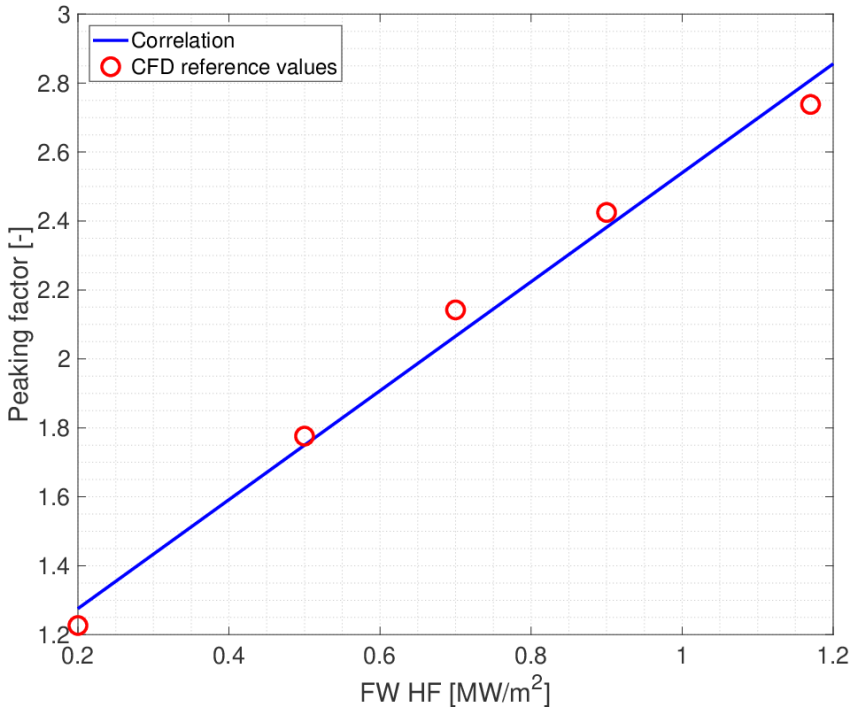

Figure 13: Correlation of the peaking factor with the FW heat flux and comparison with the values extracted from CFD.

References

[1] F. Romanelli, P. Barabaschi, D. Borba, G. Federici, L. Horton, R. Neu, D. Stork and H. Zohm, "Fusion Electricity – A roadmap to the realisation of fusion energy," European Fusion Development Agreement (EFDA), 2012, ISBN 978-3-00-040720-8T. [Online]. Available: https://www.euro-fusion.org/wpcms/wp-content/uploads/2013/01/JG12.356-web.pdf.

[2] R. Wenninger and G. Federici, "DEMO1 Reference Design - 2015 April ("EU DEMO1 2015")," EFDA_D_2LBJRY, 2015.

[3] E. Martelli, A. Del Nevo, P. Arena, G. Bongiovì, G. Caruso, P. A. Di Maio, M. Eboli, G. Mariano, R. Marinari, F. Moro, R. Mozzillo, F. Giannetti, G. Di Gironimo, A. Tarallo, A. Tassone and R. Villari, "Advancements in DEMO WCLL breeding blanket design and integration," *International Journal of Energy Research,* vol. 42, no. 1, pp. 27-52, 2017.

[4] E. Martelli, A. Del Nevo, F. Giannetti and M. Polidori, "DEMO BoP - WCLL BB PHTS and PCS preliminary design," EFDA_D_2MH7KC, 2017.

[5] L. V. Boccaccini, L. Giancarli, G. Janeschitz, S. Hermsmeyer, Y. Poitevin, A. Cardella and E. Diegele, "Materials and design of the European DEMO blankets," *Journal of Nuclear Materials,* Vols. 329-333, part A, pp. 148-155, 2004.

[6] A. Froio, C. Bachmann, F. Cismondi, L. Savoldi and R. Zanino, "Dynamic thermal-hydraulic modelling of the EU DEMO HCPB breeding blanket cooling loops," *Progress in Nuclear Energy,* vol. 93, pp. 116-132, 2016.

[7] A. Froio, F. Casella, F. Cismondi, A. Del Nevo, L. Savoldi and R. Zanino, "Dynamic thermal-hydraulic modelling of the EU DEMO WCLL breeding blanket cooling loops," *Fusion Engineering and Design,* vol. 124, pp. 887-891, 2017.

[8] A. Froio, F. Cismondi, L. Savoldi and R. Zanino, "Thermal-hydraulic analysis of the EU DEMO Helium-Cooled Pebble Bed Breeding Blanket using the GETTHEM code," *IEEE Transactions on Plasma Science,* SOFE-27 special issue, in press, 10.1109/TPS.2018.2791678, 2018.

[9] A. Del Nevo, E. Martelli, P. Agostini, P. Arena, G. Bongiovì, G. Caruso, G. Di Gironimo, P. A. Di Maio, M. Eboli, R. Giammusso, F. Giannetti, A. Giovinazzi, G. Mariano, F. Moro, R. Mozzillo, A. Tassone, D. Rozzia, A. Tarallo, M. Tarantino, M. Utili and R. Villari, "WCLL breeding blanket design and integration for DEMO 2015: status and perspectives," *Fusion Engineering and Design,* vol. 124, pp. 682-686, 2017.

[10] F. Maviglia, "DEMO PFC Heat Load Specifications," EFDA_D_2NFPNU v0.3, 2017.

[11] M. Kovari, F. Maviglia and T. R. Barrett, "DEMO 2016 - First Wall," EFDA_D_2MWN32 v1.0, 2016.

[12] A. Froio, A. Bertinetti, S. Ciattaglia, F. Cismondi, L. Savoldi and R. Zanino, "Modelling an In-Vessel Loss of Coolant Accident in the EU DEMO WCLL Breeding Blanket with the GETTHEM Code," *submitted to Fusion Engineering and Design (ISFNT13 special issue),* 2017.